

### Conclusion

Compared to the rigorous procedures<sup>2</sup> the solution to the previously stated problem, given by Eqs. (4) and (5) is approximate, but avoids the cumbersome calculations involved in the former. In this connection, the stochastic analysis of a single degree of freedom system subjected to random wind and seismic excitations to study the response characteristics was undertaken by the authors. The exciting force was assumed to be nonstationary in character, and was represented by the product of a deterministic shape function and a stationary random process characterized by its power spectral density. The choice of deterministic function and power spectral density was based on certain characteristics observed in a large number of past records of excitation process. The application of Eqs. (4) and (5) to study the peak response characteristics of the system revealed that the probability estimates for various appropriate values of  $\lambda$  are about 0.5% below those obtained by an exact procedure.

### References

- <sup>1</sup>Lin, Y.K., "Probability Distribution of Stress Peaks in Linear and Nonlinear structures," *AIAA Journal*, Vol. 1(5) 1963, pp. 1133-1138.
- <sup>2</sup>Lin, Y.K., *Probabilistic Theory of Structural Dynamics*, McGraw Hill, New York, 1967, pp. 299-304.
- <sup>3</sup>Rice, S.O., "Mathematical Analysis of Random Noise," Bell Technology, Vol. 18, 1944, p. 282 and Vol. 19, 1945, p. 46.
- <sup>4</sup>Davenport, A.G., "Note on the Distribution of the Largest Value of a Random function with Application to Gust Loading," *Proceedings of Institution of Civil Engineers*, Vol. 28, 1964, pp. 187-195.

## Finite Difference Method for Computing Sound Propagation in Nonuniform Ducts

Dennis W. Quinn\*  
Aerospace Research Laboratories,  
Wright-Patterson Air Force Base, Ohio

### Introduction

IN contrast to the analytic methods which expand solutions in a finite series of modes, the method described in this paper is that of finite differences. Numerical solutions for duct acoustics problems in two-dimensional rectangular ducts of constant cross-section have been obtained by Baumeister<sup>1</sup> for the case of no flow and by Baumeister and Rice<sup>2</sup> in the flow case. For ducts with variable cross-section, Alfredson<sup>3</sup> has used a stepped duct approach while Eversman et al.<sup>4</sup> have used the method of weighted residuals (Galerkin's Method.) A finite difference solution for a duct with variable cross-section will now be described.

### Governing Equations and Boundary Conditions

For a three-dimensional axially symmetric duct with no flow and steady state, the equations of continuity and momentum may be combined to yield<sup>1,2,7</sup>

$$\frac{\partial^2 p}{\partial z^2} + \frac{\partial^2 p}{\partial r^2} + \frac{1}{r} \frac{\partial p}{\partial r} + \left(\frac{\omega}{c}\right)^2 p = 0 \quad (1)$$

Presented as Paper 75-130 at the AIAA 13th Aerospace Sciences Meeting, Pasadena, Calif., January 20-22, 1975; submitted February 5, 1975; revision received March 21, 1975. Research accomplished while working in the capacity of a NRC Resident Research Associate.

Index category: Aircraft Noise, Powerplant.

\*Mathematician, Applied Mathematics Research Laboratory.

where  $z$  is the axial coordinate,  $r$  is the radial coordinate, and time dependence has been assumed to be of the form  $e^{i\omega t}$ . In these coordinates, the following boundary conditions are prescribed

$$p(z, r) = f(z, r) \text{ at the entrance}$$

$$(\partial p / \partial n) + i\omega / (c\zeta_r) p = 0 \text{ on the lateral boundaries}$$

$$(\partial p / \partial n) + i\omega / (c\zeta_z) p = 0 \text{ at the exit,} \quad (2)$$

where  $(\partial / \partial n)$  is the directional derivative in the direction of the outer normal to the boundary, and  $\zeta_r$  is the specific acoustic impedance of the wall lining, while  $\zeta_z$  is the specific acoustic impedance of the exit.

### Method of Solution

The well-known Riemann Mapping Theorem establishes that an arbitrary simply connected domain in the plane can be mapped conformally onto an open rectangle with vertices  $(0,1)$ ,  $(0,-1)$ ,  $(X,-1)$ , and  $(X,1)$ . (For a diagram of such a map see Fig. 1.) If the map is of the form

$$z = z(x, y); \quad r = r(x, y)$$

then for it to be conformal, the Cauchy-Riemann equations:

$$(\partial z / \partial x) = (\partial r / \partial y), \quad (\partial z / \partial y) = -(\partial r / \partial x)$$

must be satisfied. In transformed coordinates Eq. (1) becomes

$$\begin{aligned} 0 = & \frac{\partial^2 \hat{p}}{\partial x^2} + \frac{\partial^2 \hat{p}}{\partial y^2} - \frac{1}{r(x, y)} \frac{\partial z(x, y)}{\partial y} \frac{\partial \hat{p}}{\partial x} \\ & + \frac{1}{r(x, y)} \frac{\partial z(x, y)}{\partial x} \frac{\partial \hat{p}}{\partial y} \\ & + (2\pi\eta)^2 \left\{ \left[ \frac{\partial z(x, y)}{\partial x} \right]^2 + \left[ \frac{\partial z(x, y)}{\partial y} \right]^2 \right\} \hat{p} \end{aligned} \quad (3)$$

where  $\hat{p}(x, y) = p(z, r)$  and  $\eta = (1/2\pi) (\omega/c)$  is the dimensionless frequency. The boundary conditions (2) become

$$\hat{p}(0, y) = f(z(0, y), r(0, y)) = g(y) \text{ at the entrance}$$

$$\frac{\partial \hat{p}}{\partial y} = 0 \quad \text{at } y = 0$$

$$\frac{\partial \hat{p}}{\partial y} = -2\pi\eta ip \left[ \left[ \frac{\partial z}{\partial x} \right]^2 + \left[ \frac{\partial z}{\partial y} \right]^2 \right]^{1/2} / \zeta_y \quad \text{at } y = 1$$

$$\frac{\partial \hat{p}}{\partial x} = -2\pi\eta ip \left[ \left[ \frac{\partial z}{\partial x} \right]^2 + \left[ \frac{\partial z}{\partial y} \right]^2 \right]^{1/2} / \zeta_x \quad \text{at } x = X \quad (4)$$

To obtain a solution of Eqs. (3) and (4) on a cylinder, the following finite difference scheme is employed.<sup>1,2,6</sup>

Set

$$\delta x = X / (n + 1),$$

$$\delta y = 1 / (m + 1),$$

$$x_j = j \delta x, \quad j = 1, \dots, n$$

$$y_k = k \delta y, \quad k = 1, \dots, m$$

$$z_{j,k} = \partial z(x_j, y_k) / \partial y$$

$$\hat{z}_{j,k} = \partial z(x_j, y_k) / \partial x, \quad j = 1, \dots, n$$

$$r_{j,k} = r(x_j, y_k), \quad k = 1, \dots, m$$

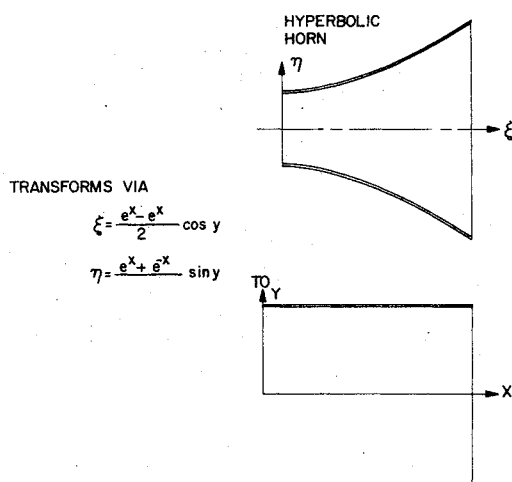


Fig. 1 Example of conformal map.

and

$$p_{j,k} = p(x_j, y_k)$$

where  $m$  and  $n$  are positive integers. Then the difference equation is

$$\begin{aligned} & (p_{j+1,k} - 2p_{j,k} + p_{j-1,k}) / (\delta x)^2 \\ & + (p_{j,k+1} - 2p_{j,k} + p_{j,k-1}) / (\delta y)^2 \\ & - (z_{j,k} / r_{j,k}) (p_{j+1,k} - p_{j-1,k}) / (2\delta x) \\ & + (\hat{z}_{j,k} / r_{j,k}) (p_{j,k+1} - p_{j,k-1}) / (2\delta y) \\ & + (2\pi\eta)^2 (\hat{z}_{j,k}^2 + z_{j,k}^2) p_{j,k} = 0 \end{aligned}$$

Collecting terms, the equation becomes

$$[2 + 2(\delta y)^2 / (\delta x)^2 - (2\pi\eta\delta y)^2 (\hat{z}_{j,k}^2 + z_{j,k}^2)] p_{j,k}$$

$$-p_{j,k+1} \left[ 1 + \frac{\hat{z}_{j,k}}{r_{j,k}} \delta y / 2 \right]$$

$$-p_{j,k-1} \left[ 1 - \frac{\hat{z}_{j,k}}{r_{j,k}} \delta y / 2 \right]$$

$$-p_{j+1,k} \left[ (\delta y)^2 / (\delta x)^2 - \frac{z_{j,k}}{r_{j,k}} \frac{(\delta y)^2}{2\delta x} \right]$$

$$-p_{j-1,k} \left[ (\delta y)^2 / (\delta x)^2 + \frac{z_{j,k}}{r_{j,k}} \frac{(\delta y)^2}{2\delta x} \right] = 0$$

$$\text{for } 1 \leq j \leq n-1, 2 \leq k \leq m-1$$

Similar expressions are obtained for  $j=n$ ,  $k=1$ ,  $k=m$ , which correspond to the boundary conditions (4).

For a reasonable number of mesh points, say 50 in the  $x$  direction and 20 in the  $y$  direction, the linear system of equations to be solved consists of 1000 unknown  $p_{j,k}$ 's to be determined. Moreover, the  $p_{j,k}$ 's are complex numbers because of the boundary conditions, so there are 2000 unknown real numbers to compute. Standard iterative methods will not work for this problem, for the system is neither positive definite nor symmetric. Therefore, a direct method<sup>5</sup> was used to solve the system, taking advantage of its sparseness. To test the method, the following example was considered.

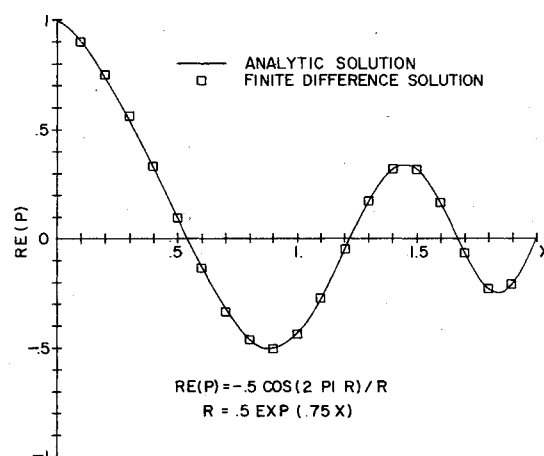
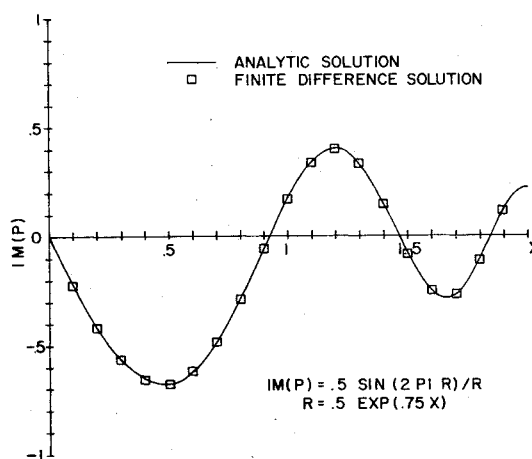
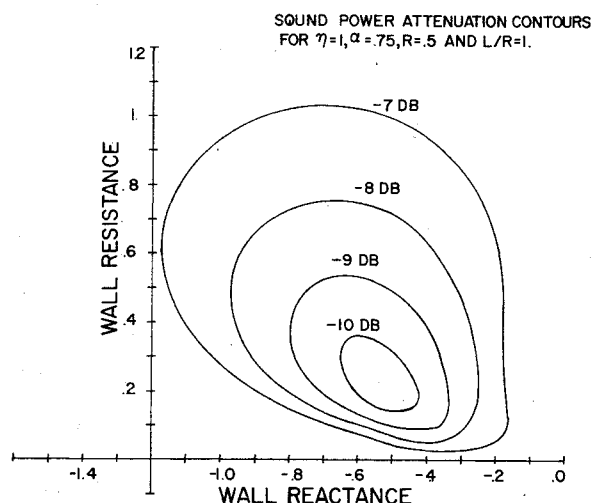
Fig. 2 Hard wall conical horn; real part of pressure vs  $x$ .Fig. 3 Hard wall conical horn; imaginary part of pressure vs  $x$ .

Fig. 4 Conical horn with uniform wall lining.

### Examples

For positive real  $\alpha$ , the cone enclosed in the  $(z, r)$  plane by the lines  $r = (\sin \alpha / \cos \alpha) z$  and  $r = (\sin \alpha / \cos \alpha) z$  and by arcs of the circles  $z^2 + r^2 = R^2$  and  $z^2 + r^2 = R^2 e^{2\alpha x}$  is the region considered. The transformation defined by

$$z = R e^{\alpha x} \cos \alpha y; \quad r = R e^{\alpha x} \sin \alpha y \quad (5)$$

maps the open rectangle onto the prescribed cone. With  $z(x,y)$  and  $r(x,y)$  defined by Eq. (5), the finite difference equations corresponding to Eqs. (3) and (4) were solved on a rectangle using the method previously described.

For short horns with slowly varying cross sections, the catenoidal and exponential horns of Morse<sup>8</sup> are approximately the same as a hyperbolic horn and a horn of the shape  $y = be^{\pi x/2D} + D$ . The agreement with Morse for these cases was extremely good; however, the restriction to slowly varying cross sections lead to solutions differing little from plane wave solutions. As an indication of the close agreement with Morse, the respective attenuation at  $x=1$  for the exponential horns were -1.9db for Morse's solution and -1.7db for the finite difference solution. It must be emphasized that the restriction to horns with slowly varying cross sections was for the purpose of approximating Morse's horn shapes and not because of limitations of the finite difference method

## Results

For a conical horn with a hard wall, the exact solution is known. For  $\alpha=0.75$ ,  $R=0.5$ ,  $\eta=1$ , and  $\rho^2 + r^2$  the solution is

$$p(z,r) = -0.5(\cos 2\pi\rho - i \sin 2\pi\rho)/\rho \quad (6)$$

In Figs. 2 and 3, the real and imaginary parts of the finite difference solution are compared to those of the exact solution (6). A study was made for the same conical horn with a uniform lining. The results are summarized in Fig. 4 where one readily sees that the best uniform lining is one with a resistance of 0.2 and a reactance of -0.5.

## Conclusion

The flexibility of the finite difference approach yields results for ducts of nonuniform cross section in the no flow case. For a hard wall, the agreement with the exact solution is outstanding. The finite difference method can also be used to compute attenuations due to nonuniform linings in both uniform and variable area ducts, as well as uniform flow in a variable area duct.

## References

- 1 Baumeister, K. J., "Application of Finite Difference Techniques to Noise Propagation in Jet Engine Ducts," NASA TM X-68261, presented at ASME Winter Annual Meeting, Detroit, Nov. 1973.
- 2 Baumeister, K. J. and Rice, E. J., "A Difference Theory for Noise Propagation in an Acoustically Lined Duct with Mean Flow," *AIAA Progress in Astronautics and Aeronautics, Aeroacoustics: Jet and Combustion Noise; Duct Acoustics*, Vol. 37, edited by H. T. Nagamatsu, MIT Press, Cambridge, Mass., 1975, pp. 435-453.
- 3 Alfredson, R. J., "The Propagation of Sound in a Circular Duct of Continuously Varying Cross-Sectional Area," *Journal of Sound and Vibration*, Vol. 23, 1972, pp. 433-442.
- 4 Eversman, W., Cook, E. L., and Beckemeyer, R. J., "A Computational Method for the Investigation of Sound Transmission in Nonuniform Ducts," *Proceedings of the Second Interagency Symposium on University Research in Transportation Noise*, North Carolina State University, Raleigh, N.C., June 1974, pp. 859-873.
- 5 Door, F. W., "The Direct Solution of the Discrete Poisson Equation on a Rectangle," *SIAM Review*, Vol. 12, 1970, pp. 248-249.
- 6 Isaacson, E. and Keller, H. B., *Analysis of Numerical Methods*, Wiley, 1966, Chap. 9.
- 7 Rice, E. J., "Attenuation of Sound in Soft-Walled Circular Ducts. Aerodynamic Noise," *Proceedings of the 1968 AFOSR-UTIAS Symposium*, University of Toronto Press, Toronto, Canada, 1969, pp. 229-249.
- 8 Morse, P. M., *Vibration and Sound*, McGraw-Hill, New York, 1948, 2nd ed., pp. 265-285.

# Calculating Starting Times for a Supersonic Nozzle Upstream of a Diaphragm

Neil McL. Barbour\*

University of the Witwatersrand,  
Johannesburg, South Africa  
and

Bradford W. Imrie†

University of Leeds, U. K.

## Nomenclature

- $a$  = speed of sound
- $A$  = cross-sectional area
- $k$  = ratio of specific heats
- $p$  = pressure
- $t = t_1 + t_2 + t_3$
- $w$  = flow velocity
- $z$  = distance from diaphragm to station  $z$  in nozzle or test section
- $\rho$  = density

## Subscripts

- $c$  = wave point  $c$
- $e$  = wave point  $e$  at station  $z$
- $D$  = diaphragm location
- $n$  = test section
- $o$  = stagnation
- $t$  = upstream of nozzle
- $x$  = upstream of stationary normal shock at station  $z$
- $y$  = downstream of stationary normal shock at station  $z$
- $z$  = downstream of moving normal shock at station  $z$
- 4 = upstream of diaphragm before rupture
- \* = nozzle throat

## Introduction

In all short duration test facilities, knowledge of the starting times is important in determining quasi-steady flow requirements. It is generally recognized<sup>1</sup> that a diaphragm downstream of the nozzle causes a longer starting time than an upstream diaphragm configuration, and hence adequate prediction of the starting times is essential for this case. A simple, experimentally verified procedure for estimating the starting times of a nozzle with a downstream diaphragm is presented herewith. The method is based upon the results (using dry air) from the Mach 1.4, 2, 3, and 4 two-dimensional nozzles of the Leeds University Supersonic Ludwig Tube.<sup>2</sup> The estimates are seen to become more accurate as the nozzle Mach number increases.

The starting process (approximated in the  $x-t$  diagram of Fig. 1) commences with the expansion wave, formed at diaphragm burst, traveling upstream through the test section and into the convergent-divergent nozzle. This wave becomes intensified with decreasing cross section (as seen from the downstream diaphragm end) and, after the throat, becomes attenuated again in the divergent part. As this rarefaction wave travels upstream it accelerates the gas in a downstream direction. Sonic velocity is first reached at the nozzle throat where the wave possesses its greatest intensity. At this instant no further part of the wave can pass upstream through the nozzle throat (since expansion waves travel at local sonic velocity). As soon as the nozzle throat becomes choked a weak

Received February 10, 1975; revision received June 20, 1975.

Index category: Nozzle and Channel Flow.

\*Lecturer in Applied Mathematics, Department of Applied Mathematics.

†Senior Lecturer in Mechanical Engineering, Department of Mechanical Engineering.